Nanohybrid silica/polymer subcritical aerogels

A. Fidalgo, L.M Ilharco, J.P.S Farinha and J.M.G. Martinho

* CQFM - Centro de Química-Física Molecular and IN - Institute of Nanoscience and Nanotechnology, Instituto Superior Técnico, Universidade Técnica de Lisboa, Av. Rovisco Pais 1, 1049-001 Lisboa, Portugal, Alexandra.fidalgo@ist.utl.pt

ABSTRACT

Novel nanohybrid silica/polymer aerogels were produced by the soft sol-gel process, under subcritical conditions. The inclusion of functionalized core-shell polymer nanoparticles (PNP) at the first stages of the sol-gel process builds up a structure stiff enough to withstand capillary pressure, yielding machineable monoliths with good mechanical properties. The influence of the silica precursor and of the size and content of the PNPs was analyzed.

Keywords: aerogels, hybrid nanocomposites, insulators

1 INTRODUCTION

The most common insulators (mineral wools and expanded polymers) are low-priced, but do not meet the demanding energetic and environmental requirements of modern industry. However, aerogels are conquering the market, so far only for high technology applications [1]. They are non-flammable, extremely light (densities in the range 3-500 $kg{\cdot}m^{-3}$), and have excellent thermal and acoustic properties (thermal conductivity in the range 0.01-0.02 $W{\cdot}m^{-1}{\cdot}K^{-1}$ and acoustic impedance 103-106 $kg{\cdot}m^{-2}{\cdot}s^{-1}$) [2]. The drawbacks of these wonder materials are their high production costs, brittleness and instability to atmospheric moisture. The present work explores the synthesis of a nanohybrid silica/polymer aerogel with improved mechanical properties, obtained at ambient pressure.

Hybrid inorganic-organic materials are the result of an intimate mixture of components, where interactions may range from van der Waals or hydrogen bonds (class *I*) to strong covalent or ionic-covalent bonds (class *II*) [3]. The sol-gel process is the best method to synthesize these materials, since the mild conditions involved are ideal to preserve the organic components [4].

Previous work proved the possibility of obtaining pure silica aerogels by subcritical drying of aged alcogels [5]. The inclusion of core-shell polymer nanoparticles (PNP) at the first stages of the sol-gel process allowed improving their mechanical properties [6-8].

In the present work, different silica precursors and PNP sizes and contents were rehearsed in view of attaining even superior properties.

2 EXPERIMENTAL

The hybrid alcogels were prepared by a two-step acid/basic catalyzed co-hydrolysis/co-condensation of a silica precursor and cross-linked core-shell particles. These consist of a trimethoxysilyl-functionalized poly(butyl methacrylate) shell and a poly(butyl methacrylate-co-butyl acrylate) core (TMS-PNP). Aqueous sodium silicate was used in alternative to tetraethoxysilane as silica precursor (Figure 1).

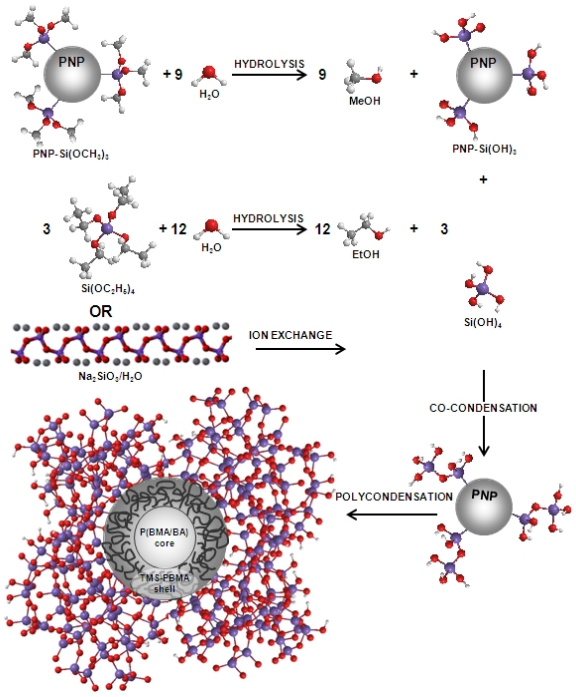

Figure 1: Reaction scheme for the synthesis of class *II* SiO_2/TMS-PNP hybrid materials.

The synthesis of the core-shell cross-linked colloidal polymer particles followed a two-stage emulsion polymerization technique. In the first stage, cross-linked seed particles were produced by batch emulsion co-polymerization of n-butylmethacrylate (BMA) and n-butylacrylate (BA), with ethylene glycol dimethacrylate (EGDMA) as cross-linker. The mixture was emulsified with sodium dodecyl sulfate (SDS), and initiated with potassium persulfate (KPS). It was then purged with nitrogen gas for 2 h, and heated to 353 K for an additional 2 h period. In the second stage, the seeds were used to prepare the PNPs, with

size and composition controlled by semi-continuous emulsion polymerization, with monomer and initiator fed under starving conditions: two mixtures (one organic and one aqueous) were independently added to the seed dispersion (purged under nitrogen) over 8 h, at constant rate, under stirring. The organic phase contained BMA, 3-trimethoxysilyl-propylmethacrylate (TMS-PMA) and EGDMA. The aqueous phase contained SDS and KPS. The reaction mixture was stirred at 353 K for an additional 2 h period before cooling to room temperature. This procedure yielded a 30 wt% solids stable dispersion of cross-linked core-shell particles with a trimethoxysilyl modified poly(butylmetacrylate) shell and a poly(butylmetacrylate-co-butylacrylate) core (TMS-PNP).

For the synthesis of the TEOS based hybrid alcogels, a mixture of TEOS, TMS-PNP and water in 2-propanol (2-PrOH) was acidified with hydrochloric acid (HCl), sealed and stirred for 1 h at 333 K, to promote the co-hydrolysis. This sol was then neutralized with ammonia (NH_4OH) and left to gel. An appropriate ageing followed at 333 K: 24 h in the mother liquor and another 24 h in a mixture of water, TEOS and 2-PrOH in the initial proportions. The aged gels were washed with 2-PrOH, and subcritically dried, at 333 K, in a *quasi*-saturated solvent atmosphere, until negligible weight loss.

For the aqueous sodium silicate based gels, the silica precursor (Na_2O:3.3 SiO_2:25.9 H_2O; d=1.37 g.cm^{-3}) was diluted to a weight percent of SiO_2 in solution of 3-10%, and ionic exchanged with Amberlite®, with different Amberlite /Na^+ mass ratios and contact periods, in order to obtain silicic acid with different pH values (1-3). The hybrid hydrogels were then obtained by catalytic condensation of silicic acid with ammonia, as used for the TEOS based alcogels. The same ageing, washing and drying procedures were used to prepare the sodium silicate based hybrid aerogels.

Hybrid silica/polymer aerogels with different TMS-PNP contents (weight percent, roughly estimated assuming full conversion of TEOS into SiO_2) and average diameters (50, 100 and 150 nm) were prepared. For comparison, pure silica aerogels were synthesized following the same procedures.

The chemical and physical properties of the dry gels have been analyzed by volume shrinkage upon drying, envelope density determinations, scanning electron microscopy (SEM), nitrogen sorption isotherms, and diffuse reflectance infrared (DRIFT) spectroscopy. The mechanical properties were measured by unidirectional compression tests, and the thermal conductivities were determined using a modified Lee's disk method.

3 RESULTS AND DISCUSSION

The inorganic aerogel is translucent, whereas the hybrid ones are opaque, even for very low polymer contents (as low as 0.5 wt%). Clearly, the presence of TMS-PNP modifies the aerogel's pore network, since the light dispersion becomes so altered.

In Figure 2 the SEM microphotographs of fracture surfaces of the inorganic and a 3 wt% TMS-PNP (100 nm diameter) hybrid silica/polymer aerogels are compared. All the samples show a bicontinuous distribution of interconnected particles and macropores, irrespective of the silica precursor and PNP content or average size, but it is clear that the inclusion of TMS-PNP (in contents as low as 0.5 wt%) is sufficient to impart a drastic change to the aerogel's microstructure: it becomes more granular, with a more uniform distribution of smaller macropores.

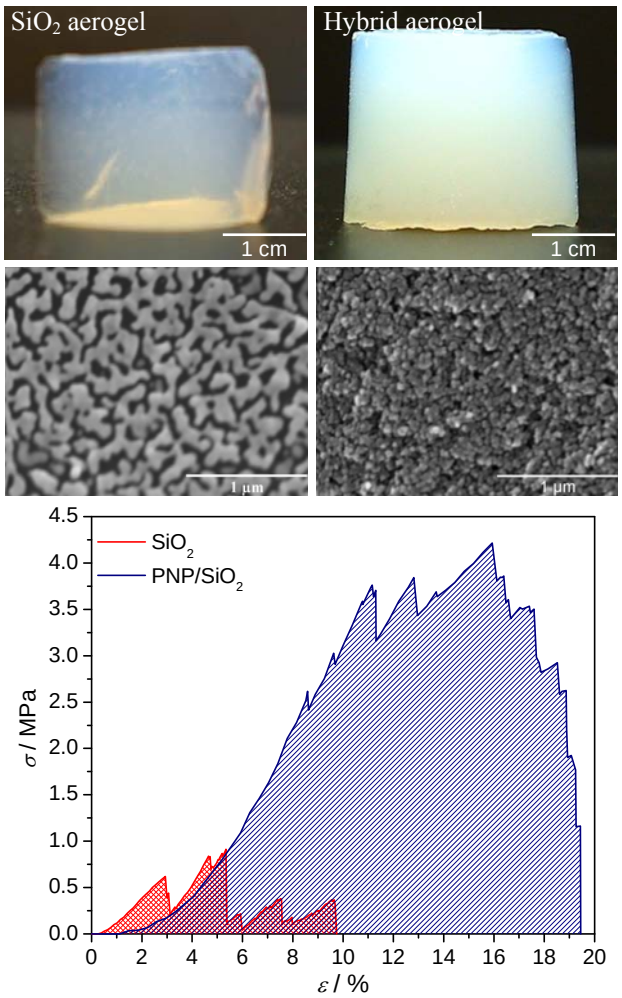

Figure 2: Photographs, corresponding cross-sectional SEM microphotographs and stress-strain curves obtained from unidirectional compression tests of a pure silica sample and a hybrid aerogel with 3 wt% PNP (100 nm).

The changes induced in the mechanical behavior of the silica aerogels by incorporation of TMS-PNP were evaluated by unidirectional compression tests. The stress-strain (σ-ε) curves in Figure 2 refer to the pure silica and the 3 wt% TMS-PNP 100 nm hybrid aerogels. The brittle nature of the silica aerogel remains upon the introduction of

TMS-PNP, as seen from the serrations along the compression curve, resulting from successive fracture of the cells' walls [9]. However, even low polymer contents promote a clear improvement in the mechanical properties of the material: the Young's modulus increases, the maximum compression strength and the corresponding strain become 3 to 5 times higher. Moreover, the improvement in the mechanical behavior is noticeable, since the hybrid aerogel is able to absorb a much higher energy (roughly the area under the σ-ε curve) up to the maximum compression strength.

The effect of the polymer content on the pore morphology of the aerogels was characterized by analysis of the N_2 adsorption-desorption isotherms, shown in Figure 3: they remain type *IV* over the entire range of polymer content, with the hysteresis loops usually associated with capillary condensation in mesopores [10]. The hysteresis is clearly type H1 for all the samples, characteristic of a uniform distribution of cylindrical mesopores. However, for the inorganic aerogel the adsorption branch is not so steep, resulting in a broader hysteresis, which points to a less defined mesopore shape.

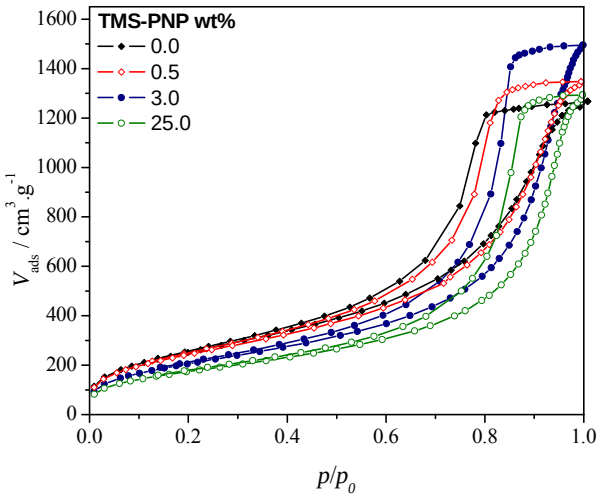

Figure 3: N_2 Adsorption-desorption isotherms (at 77 K) of the inorganic and selected hybrid aerogels with different 100 nm TMS-PNP contents.

The plateau observed at high relative pressure shows the existence of two distinct evolution trends: for low polymer contents (up to ~3 wt%), the total pore volume of the hybrid samples increases above that of the corresponding inorganic aerogel; higher polymer contents result in a decrease of the total pore volume, eventually reaching values below that of the inorganic sample.

Concurrently, for TMS-PNP contents between 0 and 3 wt%, the envelope density, ρ_e, of the aerogels decreases (from 420 to 357 kg·m^{-3}) with the increase of polymer content. This decrease reflects an increase in the percent porosity, P_r, from 80 to 83% (calculated as $100\times(1-\rho_e/\rho_s)$, taking the skeletal density, ρ_s, as 2100 kg m^{-3} [11]). Simultaneously, there is an increase of the average mesopore diameter (from 8.4 to 11.5 nm), estimated by application of the Barrett-Joyner-Halienda (BJH) method to the N_2 desorption isotherm, assuming a cylindrical pore shape [10]. On the other hand, the specific surface area (inferred from the N_2 sorption isotherms by a BET analysis of the amount of gas adsorbed at relative pressures between 0.05 and 0.3, using N_2 cross sectional area of 16.2 Å^2 [10]) decreases with increasing TMS-PNP content up to 3 wt%, from 936 to 766 m^2.g^{-1}.

The effect of the TMS-PNP average diameter on the pore morphology of the hybrid aerogels is shown in Figure 4, where the BJH pore size distribution is included in the inset.

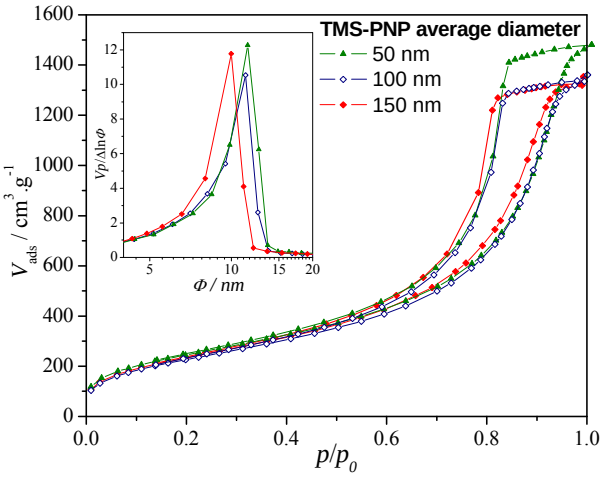

Figure 4: N_2 sorption isotherms of hybrid aerogels containing 5 wt% TMS-PNP with different sizes.

The total pore volume is similar for the 50 and 100 nm TMS-PNP hybrids, but increases when the polymer nanoparticles size is 150 nm. This increase, which corresponds to a decrease in ρ_e to 200 kg·m^{-3} (corresponding to a porosity of 89%) appears to be associated with an increase in the specific surface area and average mesopore diameter, as indicated in Table 1.

TMS-PNP size	S_{BET} (m^2/g)	V_p (cm^3/g) (p/p_0=0.99)	Φ_{BJH} (nm)
50nm	873±3	2.041514	8.15
100 nm	850±2	2.064906	8.68
150 nm	907±3	2.262190	9.32

Table 1: Surface area (S_{BET}), total pore volume (V_p) and average mesopore diameter (Φ_{BJH}) for SiO_2/5 wt% TMS-PNP hybrid aerogels with different PNP average sizes.

From these results, it is noticeable that all the synthesized aerogels possess a hierarchical bimodal pore structure, containing mesopores within the individual particles, and macropores in the interstitial voids between them. The presence of TMS-PNP, irrespectively of its

content and size, seems to promote homogeneity in the aerogel's pore network, both in the macro and mesopore ranges. A slight decrease in density (increase in porosity) may be achieved by synthesizing the aerogels with a small amount of TMS-PNP (up to ~3 wt%) with an average diameter of 150 nm. This is not due to an increase in macroporosity (which seems to decrease) but rather to the increase in the average dimensions of the mesopores, which acquire a more cylindrical shape. The same trends are observed for aerogels prepared from aqueous sodium silicate solution, with envelope densities ranging between 480 (for the inorganic aerogel) and 280 $kg \cdot m^{-3}$ (for the hybrid with 3 wt% of the 100 nm TNS-PNP).

The hybrid materials were further characterized, at the molecular structure level, by diffuse reflectance infrared (DRIFT) spectroscopy. The spectra of the inorganic aerogel and of the hybrid containing 3 wt% TMS-PNP are compared in Figure 5.

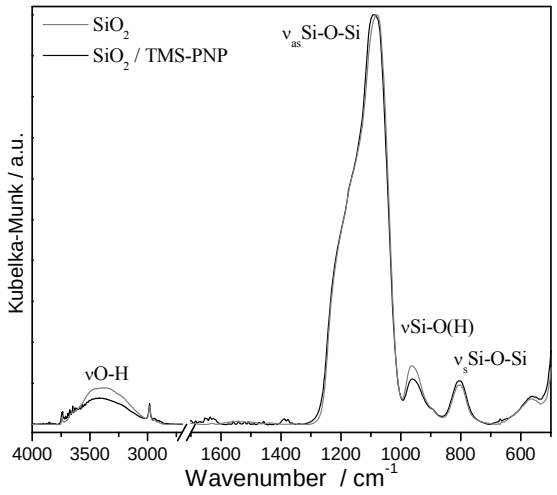

Figure 5: DRIFT spectra, normalized to the most intense band (at ~1100 cm^{-1}) of pure silica (red), and hybrid aerogel containing 3 wt% (blue) of TMS-PNP.

Both spectra present the typical features of a sol-gel silica network. The broad band centered at ~3300 cm^{-1} is assigned to the stretching mode of O-H groups involved in different hydrogen bonding. They are correlated with silanol (SiOH) groups, since there is no molecular water in these samples (the H-O-H deformation mode, expected at ~1650 cm^{-1} is absent). Another silanol band, assigned to the Si-O(H) stretching mode, appears at 950 cm^{-1}. The feature at ~800 cm^{-1} is assigned to the symmetric Si-O-Si stretching mode. The corresponding antisymmetric mode is the strongest band in the spectrum, with maximum absorption at ~1100 cm^{-1}. The similarity of this band shape in the two spectra indicates that the silica structure is not significantly altered by the presence of the polymer. The absence of the adsorbed water band and the low relative intensities of the silanol related bands are good indications that all the aerogels are relatively hydrophobic.

4 CONCLUSIONS

Nanohybrid silica/TMS-PNP aerogels were successfully produced under subcritical conditions. Aqueous sodium silicate proved to be an excellent silica precursor with cost benefits, and the size of the polymer nanoparticles was a key parameter of the aerogel's mechanical resistance. These hybrid aerogels take advantage of the synergy between organic and inorganic properties to improve the mechanical behavior of pure inorganic aerogels, still preserving their unique properties. The method developed is a green chemistry process that avoids the expensive steps of the current technologies.

REFERENCES

[1] J. E. Fesmire, Cryogenics 46, 111, 2006.

[2] L.W. Hrubesh, T.M. Tillotson, J.F. Poco *in* "Better Ceramics Through Chemistry", (Eds: C.J. Brinker D.E. Clark, D.R. Ulrich, B.J. Zelinski), Elsevier, New York 1988.

[3] C. Sanchez, B. Julián, P. Belleville, M. Popall, J. Mater. Chem. 15, 3559, 2005.

[4] N. Leventis, A. Palczer, L. McCorkle, G. Zhang, C. Sotiriou-Leventis J. Sol-Gel Sci. Tecnol. 35, 99, 2005.

[5] A. Fidalgo, M.E. Rosa, L.M. Ilharco, Chem. Mater. 15, 2186, 2003.

[6] A. Fidalgo, J.P.S Farinha, J.M.G. Martinho, M.E. Rosa, L.M. Ilharco, Chem. Mater. 19, 2603, 2007.

[7] L.M. Ilharco, A. Fidalgo, J.P.S. Farinha, J.M.G. Martinho, M.E. Rosa, J. Mater. Chem. 17, 2195, 2007.

[8] J.M.G. Martinho, L.M. Ilharco, J.P.S. Farinha, A.M. Fidalgo, P.O. Martinho, WO 2006/107226 A1; US2008/0188575 A1.

[9] L.J. Gibson, M.F. Ashby, "Cellular Solids: Structure and Properties" (2nd Ed.), Cambridge University Press, Cambridge 1997.

[10] S.J. Gregg, K.S.W. Sing, "Adsorption, Surface Area and Porosity" (2nd Ed.), Academic Press, London 1982.

[11] T. Woignier, J. Phalippou, J. Non-Cryst. Solids 93, 17, 1987.